<報 文>

An Analysis of Flow of Polymer Melts in a Screw Extruder

Chang-Dae Han

Department of Chemical Engineering, Polytechnic Institute of Brooklyn

Brooklyn, New York 11201, *U. S. A.*

Abstract

Flow of polymer melts in a screw extruder is analyzed using a viscoelastic model of a modified second-order fluid. The equations of motion are solved numerically by modifying the computational procedure advanced by Fredrickson, and the calculated extruder throughputs at various operating conditions are found to be in reasonable agreement with the experimentally observed values. Furthermore, the computational algorithm developed in the present study provides the profiles of shear rates and melt viscosity in the screw channel.

1. Introduction

In various plastic extrusion processes, molten polymer is made to flow through a wide variety of geometrical configurations. The design of flow geometry, of extrusion dies for example, is complicated by (i) the complex rheological behavior of polymeric materials and (ii) geometrical complexities. At present, the exact solution of the equations of motion with sophisticated constitutive equations is not feasible for complicated die geometries.

In the past, a considerable amount of effort has been devoted to understanding the basic nature of extrusion operations. Analyses of the flow behavior of Newtonian fluids in screw extruders were made by Carley et al (1), Carley and Srub (2) and Squires (3). Later Eccher and Valentinotti (4) reported an experimental verification of the velocity profiles predicted by the previous authors (1, 2).

In recent years, some efforts have been spent on the analysis of the flow behavior of non-Newtonian fluids in a screw extruder. These studies have used simple geometrical configurations to make the analysis more attractive. One such simplified geometry is a coaxial cylinder in which the inner cylinder is stationary. This simplification may be justified, provided that the screw channel depth is small compared to the diameter and pitch of the screw, the condition being common in plastics extruders (5). In this simplified geometry the fluid follows the combination of axial and transverse motion called "helical flow". De Haven (6) presented a procedure for designing singlescrew extruders processing pseudoplastic fluids. Colwell and Nickolls (7) and Griffith (8) analyzed the non-isothermal flow of power-law fluids in a screw extruder and compared their analytical results with experimental data. Fredrickson and Bird(9) considered the combined axial and transverse flow of the power-law fluid in an annulus. Savins (10) extended the work of Fredrickson and Bird. Tanner(11, 12) carried out experiments in helical flow using various solutions of polymethyl methacrylate and polyisobutylene.

Dierckes and Schowalter(13) also studied helical flow experimentally using polyisobutylene solution.

However, Rivlin (14) seems to have been the first who made a theoretical study of helical flow of viscoelastic fluids, using the model advanced by Rivlin and Ericksen (15). Later Fredrickson (16) extended the work of Rivlin(14). On the other hand, Coleman and Noll (17) also treated the helical flow of viscoelastic fluids, using their theory of simple fluids (18, 19) which is believed to be a more general fluid theory than that of Rivlin and Ericksen (15). In their analysis, Coleman and Noll (17) indicated that only three material functions were necessary to determine the stress and velocity profiles of helical flow.

In the present paper, a viscoelastic model of a modified second-order fluid is used to analyze the flow behavior of polymer melts in a screw extruder. Numerical solutions of the equations of motion, combined with the fluid model, generate such information as the volumetric flow rate, and the profiles of shear rates and melt viscosity in the screw channel. The calculated values of the volumetric flow rate show a reasonable agreement with the experimentally observed values.

2. Analysis

An extruder screw may be considered to consist of two sections: the melting section and the metering section (see Figure 1). In the melting section, solid polymer (in the form either of pellets or powder) is undergoing the melting process during which two phases of solid and liquid polymer coexist. In the metering section, the screw channel is filled with the completely molten polymer (one phase), which is transported by the combined action of the pressure drop across the metering section and of the rotational motion of the screw. Therefore, it may be expected that one can calculate the extruder output rates from the measurement of some pertinent variables in the melting section, the variables being the pressure drop, the screw speed, and the flow properties of the polymer melt.

Referring to Figure 1, the screw channel depth h is very small compared to the screw diameter D (see Table 1 for a specific example of a screw design). Therefore, the metering section geometry can be simply approximated by two concentric cylinders, and we confine ourselves to analyzing the steady helical flow of polymer melts between the cylinders, with the following assumptions:

Table 1. Metering Section Data (24)

Extruder Screw Diameter, D	=2.50 inches
Screw Channel Depth, h	=0.093 inches
Mean Screw Diameter, $D-h$	=2.407 inches
Fleight Width, e	=0.375 inches
Channel Width, $D-e$	=2.125 inches
Helix Angle, ϕ	=18.3 degrees
Length of Metering Section, L	=10 inches

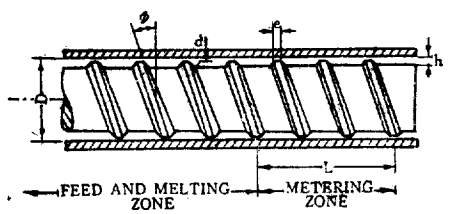

Fig. 1. Schematic Representation of Extruder Screw Metering Section

1) A uniform temperature in the screw channel (i.e., the annular space)
2) No slippage at the wall, and
3) Constant screw speed.

2.1. Equations of Motion

Consider now a polymer melt contained in the annular space between two concentric cylinders. The inner cylinder may rotate with angular velocity Ω_i while the outer cylinder may rotate with Ω_o. We will use cylindrical coordinates, with the z-axis collinear with the axis of the annular space and oriented horizontally. In addition, a pressure gradient is applied along the axis.

For this helical flow, the velocity components may be written

$$\left.\begin{aligned} V_r &= 0 \\ V_\theta &= r\omega(r) \\ V_z &= u(r) \end{aligned}\right\} \qquad (1)$$

in which $\omega(r)$, the angular velocity of a rotating cylinder and $u(r)$, the velocity component of forward movement, are a function of radial-coordinate r.

The equations of motion of a steady flow are given by

$$\left.\begin{aligned}&\frac{\partial S_{11}}{\partial r}+\frac{1}{r}(S_{11}-S_{22})=-\rho r\omega^2\\&\frac{\partial S_{12}}{\partial r}+\frac{2}{r}S_{12}=0\\&\frac{\partial S_{13}}{\partial r}+\frac{1}{r}S_{13}+\frac{\partial S_{33}}{\partial z}=0\end{aligned}\right\}\qquad(2)$$

S_{ij} are the components of the stress tensor with the subscript 1 denoting r-coordinate, 2 denoting θ-coordinate, and 3 denoting z-coordinate, respectively.

These equations may be solved subject to the boundary conditions

$$\omega(\kappa R)=\Omega_i,\quad \omega(R)=\Omega_o$$
$$u(\kappa R)=u(R)=0;\quad 0<\kappa<1\qquad(3)$$

for a given fluid model.

Here R is the radius of the outer stationary cylinder for which $\omega(R)=0$ and κR is the radius of the inner cylinder rotating with the angular velocity Ω_i.

If we assume the pressure gradient to be constant, *i, e.*,

$$-\frac{\partial S_{33}}{\partial z}=P\qquad(4)$$

integration of Eq. (2) yields

$$S_{12}=\frac{B}{r^2},\quad S_{13}=\frac{1}{2}Pr+\frac{A}{r}\qquad(5)$$

where A and B are integration constants.

2.2. The Modified Second-Order Fluid Model

In the flow of viscoelastic fluids the stress is a complicated function of the deformation rate, depending not only on the rate of deformation but also on its time derivatives (acceleration). Furthermore, the local stresses depend not only on the locol rate of strain, but also on the previous history of the liquid. The dependence of stresses on acceleration and on the past history is also typical of elastic solids. A general treatment of viscoelastic fluids is due to Coleman and Noll, who introduced the concept of a simple fluid (18, 19).

There are a large number of published papers which have discussed and suggested various forms of fluid models. However, further detailed discussion on this subject is beyond the scope of the present paper and interested readers are referred to a few recent review papers by Bogue and Doughty (20), and Spriggs et al (21). In the present study the modified second-order fluid model is chosen.

The concept of the second-order fluid was derived by Coleman and Noll (17) from the theory of simple fluids using their Retardation Theorem.

The originally suggested model has the form

$$S_{ij}=\mu_o A^{(1)}{}_{ij}+\beta A^{(1)}{}_{ik}\,A^{(1)}{}_{kj}+\gamma A^{(2)}{}_{ij}\qquad(6)$$

in which μ_o is a viscosity coefficient, β and γ are material constants, and $A^{(1)}{}_{ij}$ and $A^{(2)}{}_{ij}$ are the Rivlin-Ericksen tensor components (15) defined by

$$A^{(1)}{}_{ij}=\frac{\partial V^i}{\partial x_j}+\frac{\partial V^j}{\partial x_i}\qquad(7\text{-}1)$$

$$A^{(2)}{}_{ij}=\frac{\partial A^{(1)}{}_{ij}}{\partial t}+V^m A^{(1)}{}_{ij,m}+V^m{}_{,i}\,A^{(1)}{}_{mj}+V^m{}_{,j}\,A^{(1)}{}_{im}\qquad(7\text{-}2)$$

Interestingly enough, the form of the second-order fluid introduced by Coleman and Noll(17) is identical with the three constant model of Rivlin and Ericksen (15), which may be obtained, as a special case of the more general eight-constant model, in a simple shearing flow field. Here Eq. (6) predicts normal stress effects in simple laminar shearing flow but maintains a constant viscosity, which indicates the limited applicability of such a model. This seems to have motivated white and Metzner (22) to derive the modified form of Eq. (6), which is given by

$$S_{ij}=\bar{\mu}A^{(1)}{}_{ij}+\beta A^{(1)}{}_{ik}A^{(1)}{}_{kj}+\gamma A^{(2)}{}_{ij}\qquad(8)$$

$\bar{\mu}$ is assumed to follow the power-law:

$$\bar{\mu}=K\left[\frac{1}{2}\Pi\right]^{\frac{n-1}{2}}\qquad(9)$$

where K is the consistency index, n is the power-law constant, and Π is the second invariant of the $A^{(1)}{}_{ij}$. The material constants, β and γ, can be determined by either steady or dynamic measurement as discussed by Coleman and Markovitz (23).

It may be worth noting, however, that the choice of Eq. (9) does not have a complete theoretical justification, but it is hoped that the introduction of such a semi-empirical expression will describe both shear dependent viscosity and normal stress effects.

Given the flow field in Eq. (1), one obtains

$$\left|A^{(1)}_{ij}\right|=\begin{vmatrix}0 & r\omega' & u'\\ r\omega' & 0 & 0\\ u' & 0 & 0\end{vmatrix}\qquad(10)$$

$$\left|A^{(1)}_{ik}A^{(1)}_{kj}\right|=\begin{vmatrix}r^2\omega'^2+u'^2 & 0 & 0\\ 0 & r^2\omega'^2 & r\omega'u'\\ 0 & r\omega'u' & u'^2\end{vmatrix}\qquad(11)$$

$$\left|A^{(2)}_{ij}\right|=\begin{vmatrix}2(r^2\omega'^2+u'^2) & 0 & 0\\ 0 & 0 & 0\\ 0 & 0 & 0\end{vmatrix}\qquad(12)$$

in which $\omega'=\frac{d\omega}{dr}$ and $u'=\frac{du}{dr}$. Then, the components of the stress tensor may be obtained, substituting from Eqs. (10)—(12) into Eq. (8).

$$\left.\begin{aligned} S_{11}&=(\beta+2\gamma)Y \\ S_{12}&=S_{21}=\bar{\mu}(Y)\ r\omega' \\ S_{13}&=S_{31}=\bar{\mu}(Y)\ u' \\ S_{22}&=\beta r^2\omega'^2 \\ S_{23}&=S_{32}=\beta r\omega' u' \\ S_{33}&=\beta u'^2 \end{aligned}\right\} \tag{13}$$

in which

$$Y=r^2\omega'^2+u'^2 \tag{14}$$

Here $\bar{\mu}$ is the non-Newtonian viscosity given by

$$\bar{\mu}(Y)=K[Y] \tag{15}$$

which is a function only of r.

2. 3. Equations of Velocity Profile and Extruder Output

Use of S_{12} and S_{13} of Eq. (13) in Eq. (5) gives

$$S_{12}=\alpha/\xi^2=\xi\frac{d\omega}{d\xi}\bar{\mu}\ (Y) \tag{16}$$

and

$$RS_{13}=\frac{PR^2}{2}\left(\frac{\xi^2-\lambda^2}{\xi}\right)=\frac{du}{d\xi}\bar{\mu}(Y) \tag{17}$$

where

$$\xi=r/R$$

α and λ in Eqs. (16)—(17) may be expressed in terms of the integration constants A and B in Eq. (5).

The velocity distribution is then obtained by integrating Eqs. (16) and (17), respectively:

$$\omega(\xi)=\Omega_o-\alpha\int_\xi^1\frac{d\zeta}{\zeta^3\bar{\mu}(Y)} \tag{18}$$

$$u(\xi)=-\frac{PR^2}{2}\int_\xi^1\left(\frac{\zeta^2-\lambda^2}{\zeta}\right)\frac{d\zeta}{\bar{\mu}\ (Y)} \tag{19}$$

where Ω_o is the angular velocity of the outer cylinder. When we consider the boundary conditions at the inner cylinder:

$$\left.\begin{aligned} \omega&=\Omega_i \\ u&=0 \end{aligned}\right\} \quad \text{at } r=\kappa R \tag{20}$$

Eqs. (18) and (19) reduce to

$$\Omega_o-\Omega_i=\alpha\int_\kappa^1\frac{d\zeta}{\zeta^3\bar{\mu}(Y)} \tag{21}$$

$$0=\int_\kappa^1\left(\frac{\zeta^2-\lambda^2}{\zeta}\right)\frac{d\zeta}{\bar{\mu}(Y)} \tag{22}$$

These two equations, (21) and (22), are to be used for determining two constants, α and λ, and then the velocity profile $u(\xi)$ of Eq. (19) will be completely determined.

The volumetric flow rate, Q, is then obtained from the expression:

$$Q=\int_0^{2\pi}\int_{\kappa R}^R u(r)r\,dr\,d\theta=2\pi R^2\int_\kappa^1 u(\xi)\xi d\xi \tag{23}$$

Use of Eq. (19) in Eq. (23) gives

$$Q=-\left(\frac{P\pi R^4}{2}\right)\int_\kappa^1\frac{(\kappa^2-\zeta^2)}{\bar{\mu}(Y)}\left(\frac{\zeta^2-\lambda^2}{\zeta}\right)d\zeta \tag{24}$$

in which P is the pressure gradient across the metering section.

It is very interesting to note that the volumetric flow rate, Eq. (24), depends on K and n only of the power law model, but not on the material constats, β and γ of the flow model (8). This will make the use of Eq. (24)very convenient for practical purposes, because, in many industrially important polymer processings, shear rates are such that the flow viscosity falls in the region where the power-law model holds reasonably well. Therefore, one has no problem of obtaining the values of K and n at the practical range of shear rates, for instance by use of a capillary rheometer.

2. 4. Computational Procedure

Having derived the expressions for stress distributions (Eqs. (16) and (17)), the velocity profiles (Eqs. (18) and (19) and the extruder output (Eq. (24)), we have performed the computation with the following procedure, which is a modification of that advanced by Fredrickson (16) :

1. Assume α and λ.
2. Compute S_{12} and S_{13} from Eqs. (16) and (17) for a given value of $\xi=r/R$, where $\kappa<\xi<1.0$
3. Assume Y for the same value of ξ.
4. Compute $\bar{\mu}(Y)$ from Eq. (15).
5. Compute $Z=(S_{12}/\bar{\mu})^2+(S_{13}/\bar{\mu})^2$ with the already calculated values of S_{12} and S_{13} from step 2 and $\bar{\mu}$ from step 4. Note Z is the newly calculated Y, as may be seen from Eqs. (16) and (17).
6. Compare the assumed value $Y(\xi)$ in step 3 with the calculated value Z in step 5.
7. If the comparison in step 6 is not satisfactory, repeat the steps 3 through 6, with a newly assumed value of Y, until Z and Y converge within the predetermined margin.
8. If step 7 is completed, repeat steps 2 through 7 for all values of ξ.

9. Compute the right-hand side of Eqs. (21) and (22), respectively. Compare the computed values with the values of the left-hand sides of Eqs. (21) and (22), respectively.
10. If the comparison in step 9 is not satisfactory, assume new values of α and λ and repeat steps 2 through 9 until Eqs. (21) and (22) are satisfied.
11. If step 10 is completed, compute Q from Eq. (24).

A simplified flow diagram of the computer program is given in Figure 2.

3. Experimental Extrusion Data of Schramm(24)

For the purpose of checking the theoretical development of the present study, the author has chosen certain experimental data of Schramm (24), who ran a 2-1/2[11] nominal diameter vented type extruder,

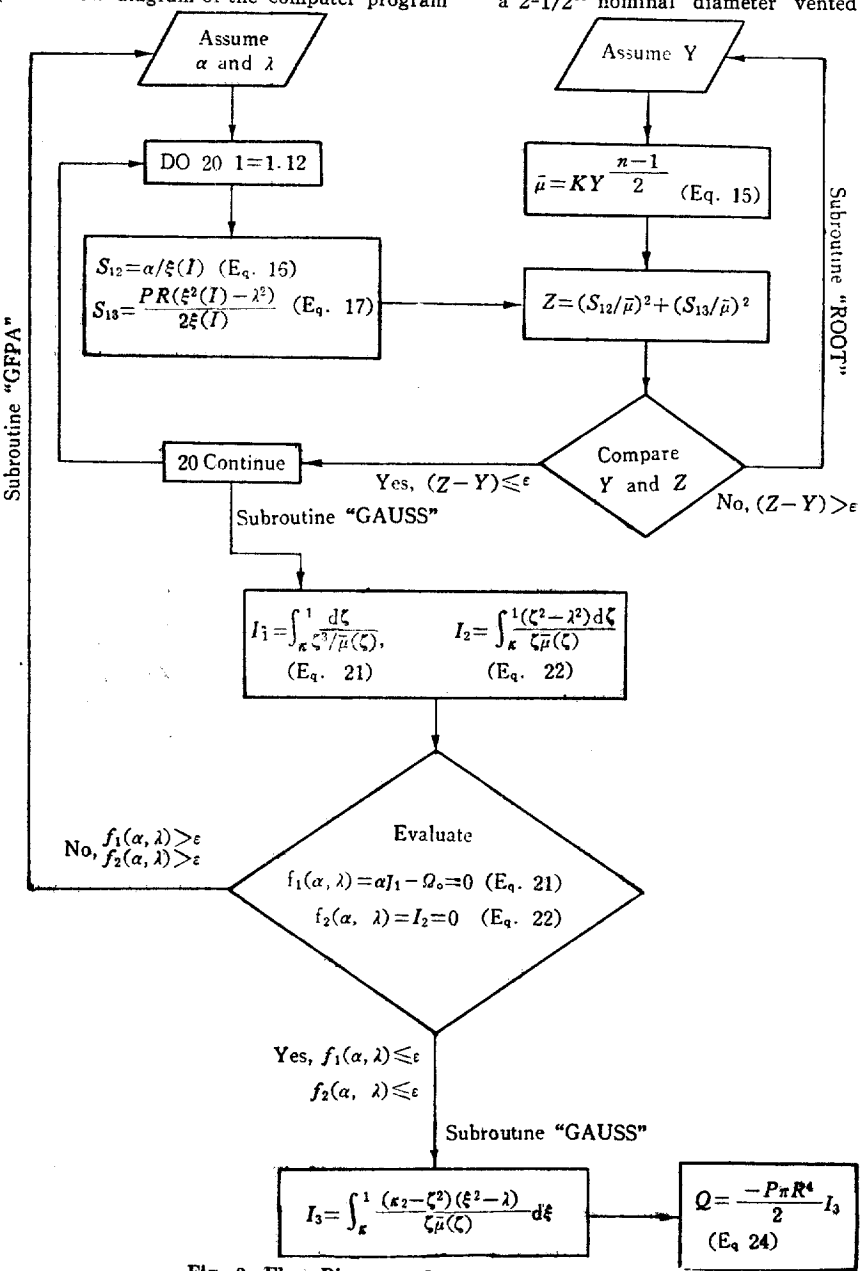

Fig. 2. Flow Diagram of the Computational Scheme

having a screw length to diameter ratio of 24 to 1. The dimensions of the metering section used for the experiment are given in Table 1.

In his experimental work, Schramm(24) used polypropylenes of a wide range of melt index(MI: 0.1～32 at 250°C), and obtained flow curves using a capillary extrusion viscometer. Figure 3 shows the shear-dependent viscosity of several samples at a temperature of 239°C, and Figure 4 shows the shear-depentdent viscosity at three different temperatures.

In the extrusion experiment, Schramm(24) measured the temperature (T) of the screw channel, the pressure drop across the metering section, ($-\Delta P$), the screw speed (N), and the volumetric extruder output (Q). In Table 2 are given three sets of his data.

Table 2. Experimental Extrusion Data of Schramm (24)

Run #	Temp., °F	$-\Delta P$, Psi	N, RPM	Q, cc/sec
10	480	300	111.0	22.6
11	480	300	126.0	24.0
23	510	550	103.2	19.7

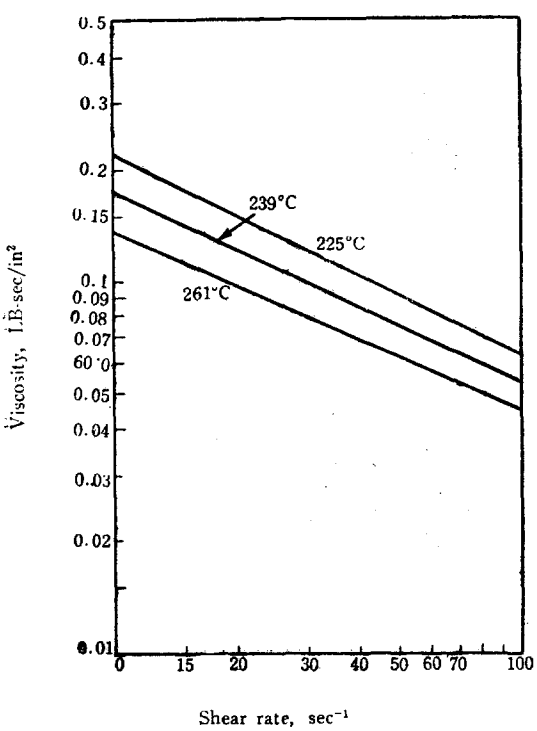

Fig. 3. Melt Viscosity vs. Shear Rate for Polypropylene at 239°C (24)

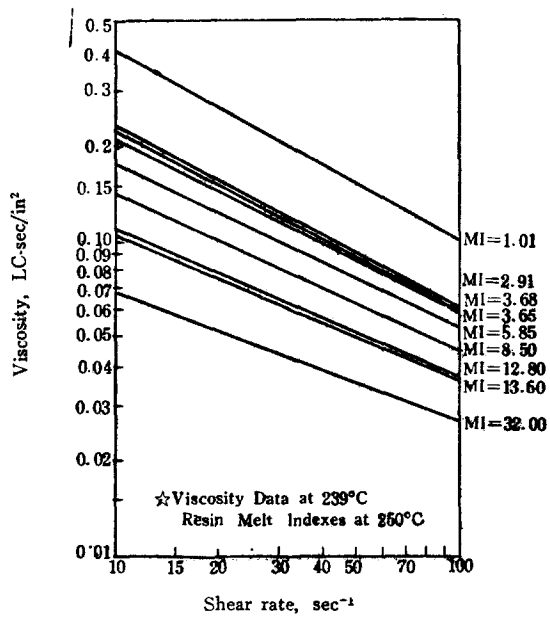

Fig. 4. Dependence of Melt Viscosity on Temperature (24)

The viscosity data in Figure 3 indicate that the polypropylene melt which was under investigation follows the power-law fluid model, in the range of shear rates indicated, thus supporting the use of Eq. (15) in conjunction with Eq. (8). The viscosity data in Figure 3 are given at 239°C, while the extrusion experiments were carried out at 480°F (249°C) for Runs no. 10 and 11 and 510°F(266°C) for Run no. 23, respectively. Consequently, an appropriate temperature correction had to be made in order to calculate K and n of Eq. (15), after calculating the flow activiation energy from Figure 4. The calculated values of K and n for the power-law model are given in Table 3. The flow index n is independent of the temperature, as may be seen from the slope of the straight lines in Figure 4, and the value of K (the

Table 3. The Values of K and n for Polypropylene Melts

Run#	Melt Index at 250°C	n	K
10	9.1	0.315	4.14×10^4 dyne $sec^{0.315}/cm^2$ at 480°F
11	9.1	0.315	4.14×10^4 dyne $sec^{0.315}/cm^2$ at 480°F
23	32.0	0.595	6.11×10^3 dyne $sec^{0.595}/cm_2$ as 510°F

flow consistency) is dependent upon the temperature.

4. Results and Discussion

A numerical computation for the extruder output Q of Eq. (24) was performed using the data given in Tables 1 and 2, by following the procedure described earlier. In actual computation, three subroutines were used: ROOT, GAUSS, and GFPA, as denoted in Figure 2. Subroutine ROOT was used to pick successive values of Y involved in the computational steps 3 through 6. sudroutine GAUSS was used to perform the necessary integrations, and subroutine GFPA was used to pick successive values of α and λ involved in the computational steps 1 through 9. The screw channel depth was divided into twelve segments ($0.96 < \zeta_i < 1.0$; $i=1, 2 \cdots\cdots 12$). This was because integration of Eq. (21), for instance, requires values of viscosity at 12 points for use in the 12 points Gauss integration method.

Table 4. Comparison of Theoretical and Experimental Values of Extruder Output

Run #	Experimental (30)	Calculated Q from the Present Study, Eq. (24)	Calculated Q from a Newtonian Fluid Model, Eq. (25).
10	22.6 cc/sec	17.32 cc/sec	31.34 cc/sec
11	24.0	20.89	35.2
23	19.7	35.46	51.5

The computed values of the extruder output Q at three different operating conditions are given in Table 4, together with the experimental values of Schramm (24). The comparison between the theoretical and experimental results for Run no. 10 and 11 are found to be in reasonable agreement. However, there are some doubts about the experimental result of Run no. 23. From the flow properties (K and n) of the polypropylene used for the experiment (see Figure 2 and Table 3), the material used for Run no. 23 is much less viscous than that used for Run no. 10 and 11 at each operating condition. Furthermore, the pressure drop across the metering section for Run no. 23 is greater than that for Run no. 10 and 11 at approximately the same screw speed. Therefore, much greater extruder outputs are expected from Run no. 23 than from Run no. 10 and 11. However, the experimental results reported by Schramm (24) are contrary to what is expected. However, the computed values confirm the expectation.

At this point it would be interesting to review a theory, proposed earlier by a few authors (1), which treats the polymer melts as a Newtonian fluid. In this theory, the extruder output is given by

$$Q=\bar{\alpha}N-\frac{\bar{\beta}\Delta P}{\eta} \tag{25}$$

where $\bar{\alpha}$ and $\bar{\beta}$ are constants determined by the screw geometry, N the screw speed, $-\Delta P$ the pressure drop across the metering section, and η the melt viscosity at the shear rate $\dot{\gamma}$ to be calculated from the expression

$$\dot{\gamma}=\frac{\pi DN}{h} \tag{26}$$

in which D is the screw diameter, h is the screw channel depth, and N is the screw speed.

The values of extruder output calculated from Eq. (25) are also given in Table 4, and they are considerably greater than those calculated from the present theory, Eq. (24). This may be due to the

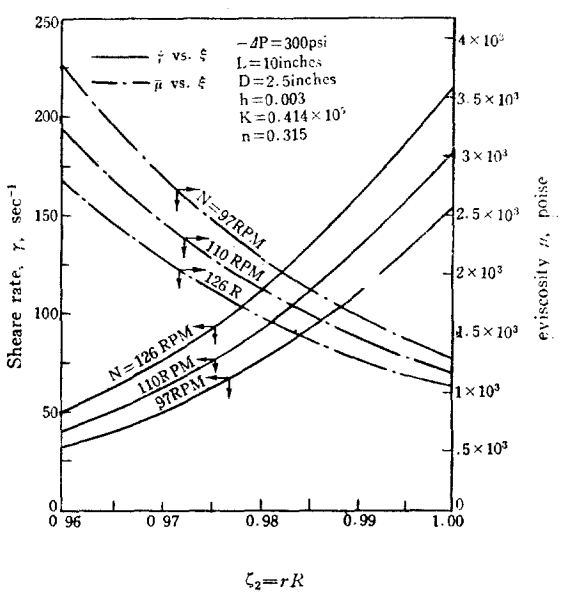

Fig. 5. Profiles of Shear Rate and Melt Viscosity in the Screw Channel with Screw Speed as a Parameter

value of the viscosity, which, in turn, is due to the value of shear rate calculated from Eq. (26). Note,

however, that shear rates in the screw channel vary significantly from the surface of the screw to the surface of the barrel.

Because of the helical nature of the flow pattern in the screw channel, the shear rate near the moving surface is expected to be greater than that near the stationary surface. The profiles of the shear rate, together with the profiles of melt viscosity in the screw channel, are given in Figure 5, with the screw speed as a parameter. Note that the shear rates are calculated here from the combination of the forward and angular motion, as seen from Eq. (14), while Eq. (26) depends only on the angular motion.

Since the polymer melt viscostiy is clearly shear-dependent, as seen from Figures 3 and 4, the viscosity near the moving surface would be less than that near the stationary surface. In Figure 6 are shown the profiles of the shear rate and the melt viscosity in the screw channel computed from Eqs. (14) through (22), with the pressure drop across the metering section as a parameter.

To summarize, the analysis presented in this paper gives a deeper insight into the flow behavior of polymer melts in the metering section of a screw extruder. A computational procedure is advanced and demonstrated for obtaining the extruder output, and the profiles of the shear rate and melt viscosity in the screw channel. The theoretically predicted extruder output is found to be in reasonable agreement with the experimental data.

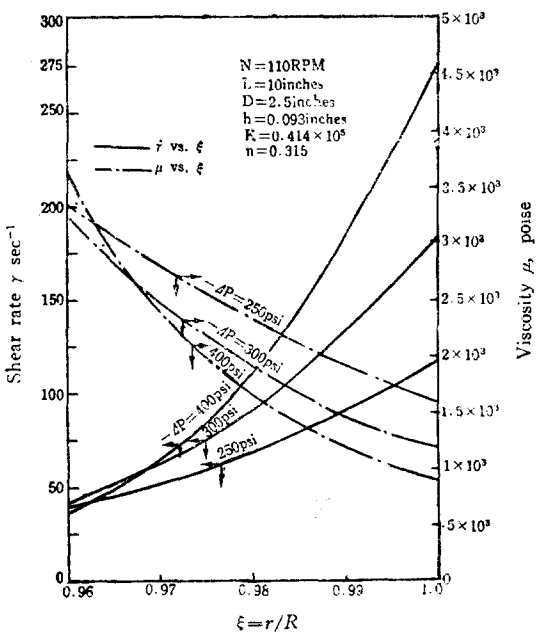

Fig. 6. Profiles of Shear Rate and Melt Viscosity in the Screw Channel with Pressure Drop as a Parameter

Nomenclature

A: Integration constant defined by Eq. 5

$A^{(1)}_{ij}$: Rivlin-Erickson tensor components defined by Eq. 7-1

$A^{(2)}_{ij}$: Rivlin-Erickson tensor components defined by Eq. 7-2.

B: Integration constant defined by Eq. 5

D: Screw diameter

h: Screw channel depth

K: Consistency Index

N: Screw speed

n: Power-law constant

P: Pressure gradient

Q: Volumetric flow rate

R: Radius of the outer cylinder

S_{ij}: Components of the stress tensor

u: Velocity component of forward movement

V_i: Components of velocity

Y: Quantity defined by Eq. 14.

$\bar{\alpha}$: Constant

$\tilde{\alpha}$: Constant determined by the screw geometry

β: Constant defined by Eq. 6

$\tilde{\beta}$: Constant determined by the screw geometry

γ: Constant defined by Eq. 6.

$\dot{\gamma}$: Shear rate

M: Melt Viscosity

κ: Ratio of the radius of the inner cylinder to that of the outer cylinder

λ: Constant

μ_0: Viscosity coefficient

$\bar{\mu}$: Non-Newtonian viscosity

ξ: Dimensionless radial variable, r/R

Π: Second invariant of $A^{(1)}_{ij}$

Ω_i: Angular velocity of the inner cylinder

Ω_o: Angular velocity of the outer cylinder

ω: Angular velocity.

References

1. Carley, J. F., Mallouk, R. S. and Mckelvey, *J. M.*, *Ind. Eng. Chem.* **45** 974 (1953).
2. Carley, J. F. and Strub, R. A., *Ind. Eng. Chem.* **45**, 978 (1953).
3. Squires, P. H., *SPE J.* **14**, 24 (1958).
4. Eccher, S. and Valentinotti, A., *Ind. Eng. Chem.* **50**, 829 (1958).
5. Mckelvey, J. M., *Polymer Processing* John Wiley and Sons, Inc. (1962).
6. DeHaven, E. S., *Ind. Eng. Chem.* **51** 813 (1959).
7. Colwell, R. E. and Nickolls, K. R., *Ind. Eng. Chem.* **51**, 841 (1959).
8. Griffith, R. M., *I & EC Fundamentals* **1**, 180 (1962).
9. Fredrickson, A. G. and Bird, R. B., *Ind. Eng. Chem.* **50**, 347 (1958).
10. Savins, J. G., *Trans. AIMB* **213**, 325(1958).
11. Tanner, R. I., *Chem. Eng. Sci.* **19**, 349(1964).
12. Tanner, R. I., *Rheol. Acta.* **3**, 26 (1963).
13. Dierckes, A. G. and Schowalter, W. R., *I & EC Fundamentals* **5**, 263 (1966).
14. Rivlin, R. S., *J. Rat. Mech. Anal.* **5**, 179 (1956).
15. Rivlin, R. S. and Ericksen, J. F., *J. Rat. Mech. Anal.* **4**, 323 (1955).
16. Fredrickson, A. G., *Chem. Eng. Sci.* **11**, 252 (1960).
17. Coleman, B. D. and Noll, W., *J. Appl. phys.* **30**, 1508 (1959).
18. Coleman, B. D, and Noll, W., *Arch. Rat. Mech. Anal.* **3**, 289 (1959).
19. Noll, W., *Arch. Rat. Mech. Anal.* **2**, 197 (1958).
20. Bogue, D. C. and Doughty, J. O., *I & EC Fundamentals* **6**, 388 (1967).
21. Spriggs, T. W., Huppler, J. D. and Bird, R. B., *Trans. Soc. Rheol.* **10**, 191 (1966).
22. White, J. L. and Metzner, A, B., *A. I. Ch. E. Journal* **11**, 324 (1965).
23. Coleman, B. D. and Markovitz, H., *J. Appl. phys.* **35**, 1 (1964),
24. Schramm, C. K., *MS Thesis* (*Ch. E.*), Polytechnic Institute of Brooklyn. 1961.